JICE - Journal of Infrastructure and Civil Engineering
Vol. 6, No. 3, (Nov, 2026),
pp. 314-328

Article submitted : 10 09 2026
Review accepted : 04 11 2026
Online Published : 10 11 2026

JICE
JOURNAL OF INFRASTRUCTURE AND CIVIL ENGINEERING
Web: http://jice.sttp-yds.ac.id/index.php/jice/index
ISSN: 2809-5030 (online) 2809-5227 (print)



Seismic Performance and Structural Capacity Assessment of a Ten-Story Reinforced Concrete Building Using Nonlinear Static Pushover Analysis

Cut Mutia Rani[1*], Trimailuzi[2], Mena Fadillia Lukman[2], Melvi Maulita Napitupulu[1], Khairunnisa[3], Wisnu Prayogo[4]

[1]*Construction Management Study Program, Universitas Negeri Medan, Indonesia*
[2]*Building Engineering Education Study Program, Universitas Negeri Medan, Indonesia*
[3]*Architecture Study Program, Universitas Negeri Medan, Indonesia*
[4]*Environmental Engineering Study Program, Universitas Negeri Medan, Indonesia*

[*]*cutrani@unimed.ac.id*

Abstract

The seismic performance of reinforced concrete buildings depends on adequate structural strength and the ability to sustain lateral deformation beyond the elastic range. This study evaluates the structural capacity and seismic performance of a ten-story reinforced concrete building by integrating linear structural assessment with nonlinear static pushover analysis. The evaluation considers modal characteristics, mass participation, interstory drift, beam and column capacities, pushover capacity curves, plastic hinge development, and seismic performance levels in the X and Y directions. The modal analysis incorporates twelve vibration modes, achieving cumulative translational mass participation ratios of 94.13% and 94.08% in the X and Y directions, respectively. The beam capacity assessment indicates a nominal flexural strength of 186.96 kN·m against a factored moment demand of 64.92 kN·m, while the evaluated column exhibits a reduced axial capacity of 6407.29 kN against an axial demand of 1627.27 kN. The pushover analysis reveals maximum base shear capacities of 17,110.19 kN at a roof displacement of 0.715 m in the X direction and 16,301.71 kN at 0.699 m in the Y direction, indicating approximately 5.0% greater lateral resistance in the X direction. Plastic hinges progressively develop predominantly within the lower and intermediate stories as lateral displacement increases. The ATC-40 capacity spectrum assessment identifies performance-point base shears of 14,944.62 kN and 14,907.81 kN in the X and Y directions, respectively. Both directions are classified within the Damage Control (SP-2) performance level, situated between Immediate Occupancy (SP-1) and Life Safety (SP-3). These findings indicate that the investigated building possesses adequate structural member capacity and maintains lateral resistance under the evaluated seismic demands, while exhibiting moderate directional differences in nonlinear deformation response.

Keywords: *reinforced concrete building; seismic performance; structural capacity; nonlinear static analysis; pushover analysis; plastic hinge; ATC-40.*

1. Introduction

Reinforced concrete (RC) buildings in seismic regions require assessment methods that can identify global lateral response and local member demand beyond the elastic range.

https://doi.org/10.35583/jice.v6i3.240

Linear analysis remains useful for routine design. It does not directly describe stiffness degradation, force redistribution, plastic-hinge formation, or displacement at a selected performance state. Recent nonlinear studies show that these response quantities can vary markedly even among buildings with comparable structural systems. Encalada et al. (2026) examined two existing RC frame–flat-slab buildings and reported maximum interstory drifts of 3.6% under BSE-1E and 8.8% under BSE-2E. Under BSE-2E, instability occurred when the stability coefficient exceeded 0.33 and lateral strength loss surpassed 20%. Displacement demands were about twice the corresponding capacities. Up to 20% of beams and 10% of columns exceeded the adopted damage thresholds. Repapis (2016) performed more than 1000 nonlinear analyses on five- and seven-story RC buildings. The study included incremental dynamic analyses with 15 ground-motion records and showed that nonlinear static estimates could remain within the range of dynamic predictions yet differ substantially from their mean values. Zameeruddin and Sangle (2021) evaluated 15 RC moment-resisting frames. The frames covered five building heights: 4, 6, 8, 10, and 12 stories. Each height was modeled with one, three, and five bays. Story height was 3 m and bay length was 4 m. For the four-story three-bay frame, base shear reached 333.21 kN under a uniform pattern and 240.16 kN under the code-based pattern, while roof displacement remained close at 26.6 and 26.2 cm for these cases.

Nonlinear static pushover analysis is widely used because it represents structural yielding through a capacity curve of base shear versus control-node displacement. The procedure permits inspection of hinge sequence and deformation demand. Its reliability still depends on lateral-load distribution and higher-mode effects. Krawinkler and Seneviratna (1998) showed that pushover analysis can estimate inelastic strength and deformation demands but may become inadequate when a fixed load pattern cannot reproduce the governing dynamic response. Fazarinc et al. (2024) represented pushover response by a trilinear model governed by 12 structural parameters. The model was applied to 109 university buildings covering more than 300,000 m^2. The existing stock had one-half the limit-state peak-ground-acceleration capacity of the new-building scenario. Numerical representation also affects predicted response. Zendaoui et al. (2016) compared four nonlinear modelling approaches against a four-story RC frame test. Force-based formulations required at least four integration points; five points produced stabilized predictions. Displacement-based formulations required at least four elements for acceptable accuracy. ATC-40 applications show how a capacity curve is translated into a performance level. Pierre and Hidayat (2020) classified the X- and Y-direction responses as Immediate Occupancy because the maximum drift of 0.00047 remained below the adopted 0.005 limit. Safarizki et al. (2013) reported target displacements of 0.188 m in the X direction and 0.132 m in the Y direction for an existing RC building using 19.3 MPa concrete and 320 MPa reinforcement steel. Its initial response was classified between Life Safety and Collapse Prevention. Steel bracing reduced target displacement by approximately 16–55%.

Building height and floor system influence lateral stiffness and displacement demand. Member strength and stiffness distribution also affect the relationship between lateral resistance and deformation. A pushover result is therefore more informative when it is interpreted together with modal properties, interstory drift, and member capacity checks. Abd-Elhamed et al. (2023) evaluated 5-, 10-, and 15-story RC buildings with solid-slab, hollow-block, and flat-slab systems. For the 10-story models, the reported base-shear coefficients were 0.090, 0.063, and 0.055 for the three floor systems. Peak roof-drift ratios reached 0.78%, 1.00%, and 1.35%. Relative to the solid-slab model, the hollow-block and flat-slab models developed roof-drift ratios that were about 22% and 73% higher. Ariyanto et al. (2026) studied 8-, 10-, and 12-story RC special moment-resisting frames with the same total height of 30 m. The 12-story configuration had a natural period of 1.559 s and a base-shear capacity of 8722 kN. The eight-story model reached the largest drift ratio of 1.072%, while all three models were classified at the Life Safety performance level. These findings show that story number or base-shear capacity alone does not describe seismic performance. The

present study assesses a ten-story RC building by integrating structural capacity evaluation with nonlinear static pushover response in the principal X and Y directions. The assessment includes modal characteristics and base reaction. It examines story drift, stiffness, beam and column capacity, base-shear–displacement curves, plastic-hinge development, and the ATC-40 performance point so that global seismic demand and local resistance are evaluated within the same analytical framework.

2. Methodology

2.1. Structural Model and Linear Seismic Assessment

The ten-story reinforced concrete building was represented using a three-dimensional analytical model developed in SAP2000 (Computers and Structures, Inc., CSI) to evaluate its elastic seismic characteristics before the nonlinear assessment. The software was employed to perform both linear structural analysis and nonlinear static pushover analysis within a consistent numerical modeling framework. The linear assessment included modal analysis, base reactions, response-spectrum analysis, and interstory displacement evaluation in the two principal horizontal directions. Twelve vibration modes were extracted, and the cumulative translational mass participation ratios were verified against the adopted minimum requirement of 90% in both the X and Y directions. Modal periods and mass participation ratios were evaluated to identify the dominant translational and torsional characteristics of the structural system. Static seismic and response-spectrum load cases were analyzed separately to compare their corresponding base shear values. The dynamic base shear was required to reach at least 85% of the static base shear. When this criterion was not satisfied, the response-spectrum results were adjusted using a scale factor calculated from the ratio of 0.85Vstatic to Vdynamic. Interstory displacements were obtained from the SAP2000 response-spectrum analysis at representative floor joints. A typical story height of 3800 mm was adopted for drift evaluation, together with a deflection amplification factor (Cd) of 5.5 and an importance factor (I) of 1.0. The allowable interstory displacement was set at 95 mm. The linear analysis established the initial structural stiffness, modal characteristics, lateral-force demands, and deformation profiles, providing a reference for evaluating the subsequent nonlinear capacity and plastic-hinge response.

2.2. Structural Member Capacity Assessment

Structural member capacity was evaluated separately for representative reinforced concrete beam and column sections to determine whether the gravity and seismic force demands remained below the calculated section strengths. The beam assessment used a rectangular section with a width of 350 mm, an overall depth of 600 mm, and a span of 6000 mm. The specified concrete compressive strength was 35 MPa, while the longitudinal reinforcement yield strength was 420 MPa. A strength-reduction factor of 0.90 was adopted in the flexural calculation. The effective depth, reinforcement ratio, minimum steel area, provided reinforcement area, neutral-axis depth, and equivalent compression-block depth were calculated in sequence. The flexural demand used in the calculation was 64.92 kN·m. The nominal moment strength was obtained from force equilibrium between the tensile reinforcement and the concrete compression block, and the resulting section strength was compared directly with the applied factored moment. Column capacity was assessed using a 750 mm by 750 mm section with a concrete compressive strength of 35 MPa and reinforcement yield strength of 420 MPa. The evaluated column demand consisted of an axial load of 1627.274 kN, a bending moment of 186.61 kN·m, and a shear force of 44.312 kN. Axial-flexural behavior was checked through eccentricity, balanced axial strength, required nominal strength, reinforcement area, strain compatibility, and the Whitney equivalent stress block. A strength-reduction factor of 0.65 was applied to the axial resistance.

Column shear resistance and transverse reinforcement spacing were also checked. The member calculations followed reinforced concrete strength provisions in SNI 2847:2019.

2.3. Nonlinear Static Pushover and Performance Assessment

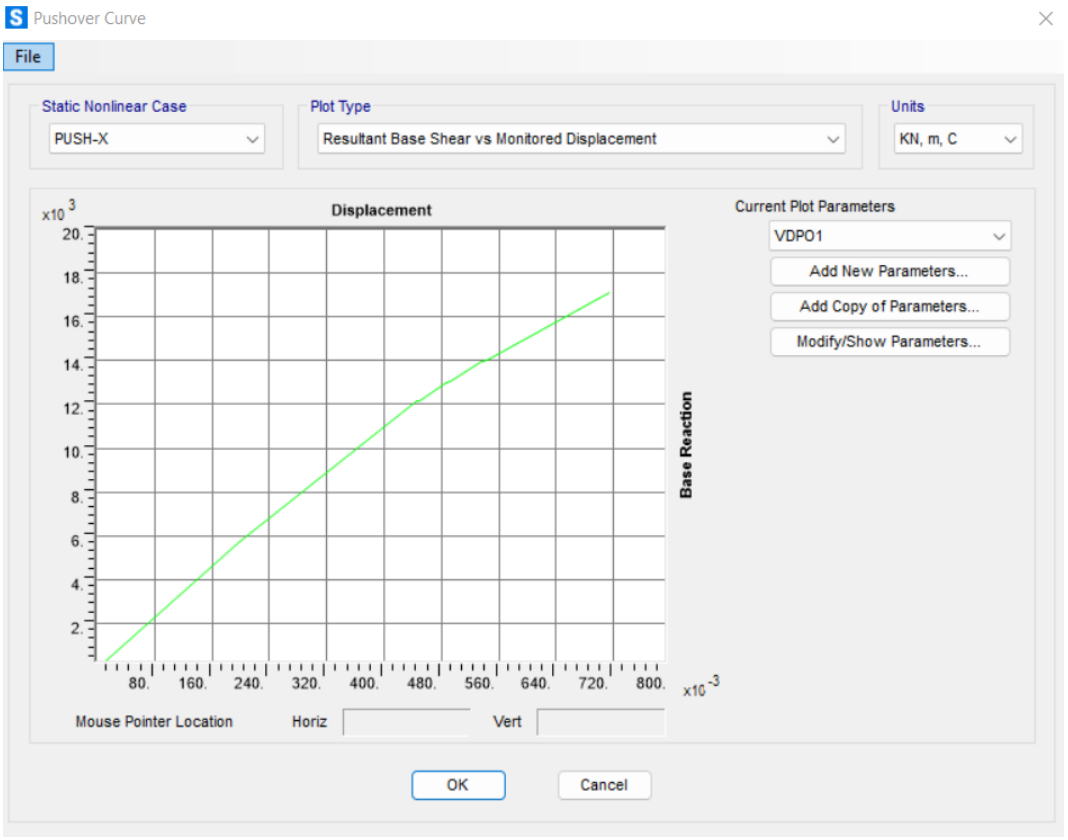
Nonlinear static pushover analysis was performed using SAP2000 independently in the X and Y directions to evaluate the lateral load-carrying capacity and progression of inelastic structural behavior. Two nonlinear load cases, PUSH-X and PUSH-Y, were considered. Lateral loads were incrementally increased while the displacement of the control point and corresponding total base shear were recorded at each converged analysis step. The resulting pushover capacity curves were expressed as relationships between base shear and monitored displacement. Plastic-hinge development was evaluated using the performance ranges A–B, B–IO, IO–LS, LS–CP, CP–C, C–D, D–E, and Beyond-E to identify the sequence of yielding and redistribution of inelastic demands. Eight nonlinear analysis steps were obtained for the X direction, while ten steps were obtained for the Y direction. Structural performance was subsequently evaluated using the ATC-40 Capacity Spectrum Method implemented through the SAP2000 nonlinear analysis results. The pushover capacity curves were transformed into spectral acceleration–spectral displacement coordinates and compared with the seismic demand spectrum to determine the performance point. The corresponding displacement was normalized relative to the structural height to evaluate the global deformation response and interpret the structural performance level according to ATC-40 criteria, including Immediate Occupancy (SP-1), Damage Control (SP-2), and Life Safety (SP-3). The nonlinear results were integrated with the previously evaluated modal characteristics, interstory drifts, base shear demands, and member capacities to assess global lateral resistance, deformation demands, plastic-hinge progression, and section-level structural performance. Differences between the X and Y directions were evaluated to characterize the directional dependence of the building's seismic response.

3. Results and Discussion

3.1. Lateral Load-Carrying Capacity and Pushover Response

As shown in Figure 1, the pushover capacity curves describe the relationship between resultant base shear and monitored control-point displacement for loading in the principal X and Y directions. The X-direction response reaches a maximum base shear of 17,110.19 kN at a displacement of 0.7146 m, whereas the Y-direction response reaches 16,301.71 kN at 0.6992 m. The maximum lateral resistance in the X direction is therefore about 5.0% higher than that in the Y direction, while the corresponding maximum displacement is about 2.2% larger. At the first loaded step, the secant stiffness calculated from the base shear-to-displacement ratio is approximately 29.1 MN/m for PUSH-X and 27.7 MN/m for PUSH-Y, indicating a directional stiffness difference of about 4.8%. At the final point, these ratios decrease to approximately 23.9 and 23.3 MN/m, respectively. This reduction is consistent with progressive loss of effective lateral stiffness as reinforced concrete members enter the inelastic range. Krawinkler and Seneviratna (1998) described the base shear–roof displacement curve as a direct representation of strength and deformation response, while also emphasizing that the reliability of conventional pushover analysis depends on how well the selected lateral load pattern represents the governing dynamic response. Zameeruddin and Sangle (2021) similarly showed that lateral load distribution can materially change the capacity curve; for their four-story three-bay RC frame, ultimate base shear varied from 240.16 to 333.21 kN although the associated roof displacement remained close to 26.2–26.6 cm. This further confirms that the system exhibits modest asymmetry while maintaining broadly comparable nonlinear response characteristics under both loading directions.

A



B

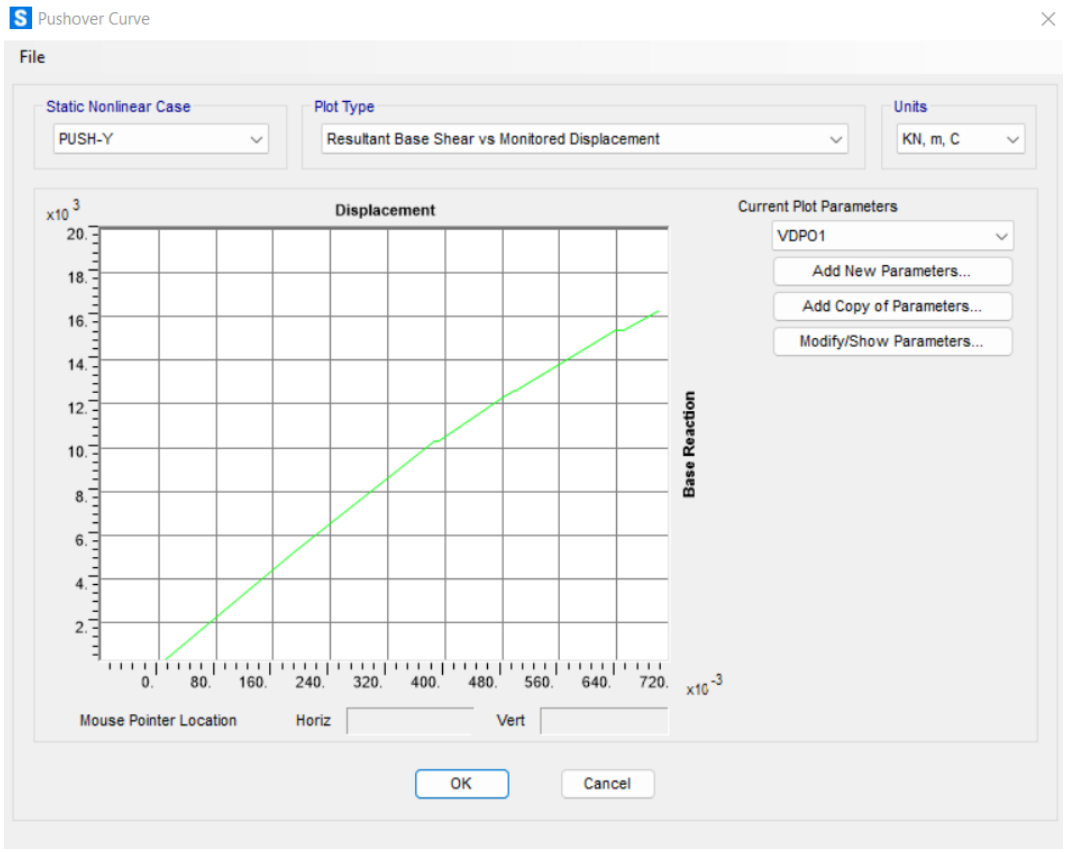


Figure 1. Pushover capacity curves of the ten-story reinforced concrete building: (a) pushover response in the X direction and (b) pushover response in the Y direction

The shape of Figure 1 also shows that the structural response is not governed by a single constant stiffness over the full displacement range. The increase in base shear becomes less proportional to displacement at the larger analysis steps, which suggests redistribution of internal forces and progressive nonlinear action. This trend is more evident in the Y direction, where the numerical output includes reductions in base shear from 12,376.89 to 12,318.24 kN and from 12,634.58 to 12,618.75 kN while displacement continues to increase. These reductions are approximately 0.47% and 0.13%, respectively, and should be interpreted as local changes in the global resistance path rather than as an immediate indication of collapse. Repapis (2016), based on more than 1000 nonlinear analyses of existing RC buildings, reported that pushover capacity curves provide useful estimates of initial stiffness, maximum strength, and global yield displacement, although target displacement estimates can differ from the mean response obtained through incremental dynamic analysis. For one investigated building, pushover target displacement ranged from 6.5 to 9.2 cm, compared with a dynamic-analysis range of 2.8–10.0 cm and a mean of 6.0 cm. Abd-Elhamed et al. (2023) also demonstrated the sensitivity of lateral response to structural stiffness in ten-story RC buildings; normalized base shear coefficients of 0.090, 0.063, and 0.055 were reported for solid, hollow-block, and flat-slab systems, with pushover roof drift ratios of 0.78%, 1.00%, and 1.35%. Fazarinc et al. (2024) further treated load-bearing strength and deformation capacity as distinct but coupled parameters of the pushover curve, supporting interpretation of the present X–Y difference through both resistance and displacement rather than maximum base shear alone.

3.2. Plastic Hinge Development under X-Direction Pushover Loading

Figure 2(a–h) shows the progressive development of plastic hinge states in the ten-story reinforced concrete building during X-direction pushover loading from Step 1 to Step 8. At Step 1, shown in Figure 2(a), the structural members remain predominantly within the initial response range, with no extensive development of advanced hinge states. Plastic hinge activation becomes more apparent at Step 2 in Figure 2(b), particularly within the lower and intermediate stories. The number of activated hinge locations increases through Steps 3 and 4, as presented in Figure 2(c) and Figure 2(d). The upper stories exhibit less pronounced nonlinear activity during these stages. This distribution indicates that inelastic demand develops first within the lower portion of the structural system, where larger story shear and overturning effects are generally expected under lateral loading. Zhao et al. (2011) explained that plastic deformation in reinforced concrete flexural members tends to localize within limited regions after yielding, which subsequently control the deformation capacity of the members. Zhang et al. (2018) also reported that the progression of plastic hinges provides a useful indicator of structural nonlinearity during pushover loading. Their investigation of a six-story reinforced concrete frame showed that changes in member properties affected the location and progression of both beam and column hinges. The response shown in Figure 2(a–d) therefore provides a local representation of the onset and spatial development of nonlinear behavior that complements the global base shear–displacement response discussed in Section 3.1.

At the later loading stages, Figure 2(e–h) shows a broader distribution of activated plastic hinges across the lower and intermediate portions of the structural frame. Figure 2(e) and Figure 2(f), corresponding to Steps 5 and 6, indicate that several hinge locations have progressed beyond their initial states as the monitored displacement increases. This progression becomes more visible in Figure 2(g) and Figure 2(h), representing Steps 7 and 8. Several hinge markers in the lower stories develop toward the IO–LS range, while the upper stories retain fewer advanced hinge states. No visually identifiable hinge in Figure 2 reaches the LS–CP, CP–C, C–D, D–E, or Beyond-E ranges at the displayed analysis stages. Hussein et al. (2021) reported a comparable tendency in reinforced concrete frames, where plastic hinges were concentrated mainly in the lower portions of the structures and fewer hinges developed in the upper stories.

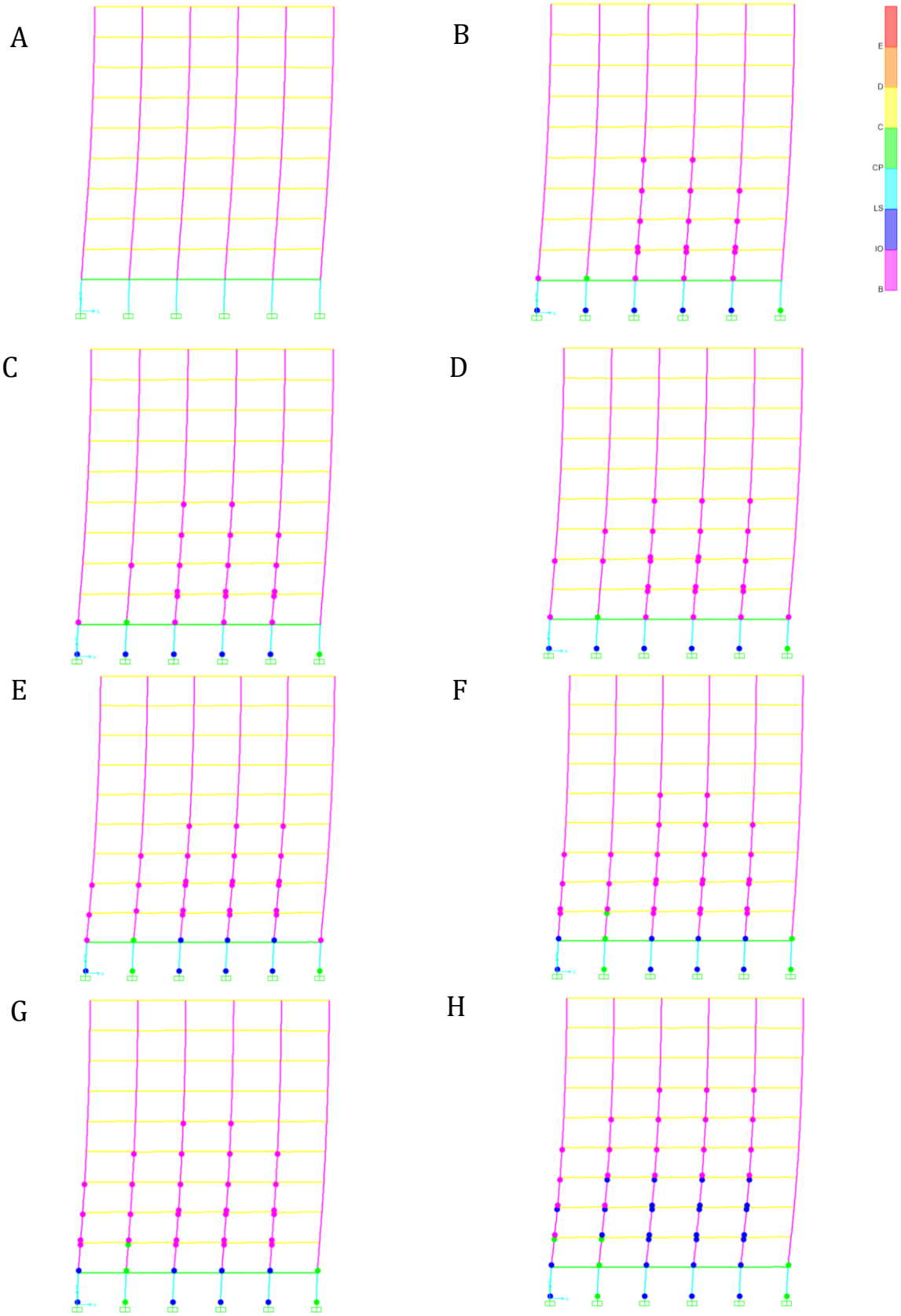


Figure 2. Evolution of plastic hinge states in the ten-story reinforced concrete building under nonlinear static pushover loading in the X direction: (a) Step 1, (b) Step 2, (c) Step 3, (d) Step 4, (e) Step 5, (f) Step 6, (g) Step 7, and (h) Step 8.

Mitropoulou et al. (2022) also showed that hinge-state distributions can remain within the B–IO and IO–LS ranges even after extensive nonlinear response develops. In their strengthened RC system, 35 hinges were obtained under uniform negative X-direction loading, including 10 hinges within B–IO and 25 within IO–LS. Le and Pham (2024) further demonstrated that plastic-hinge modelling assumptions influence nonlinear static predictions, with differences of approximately 1.26–2.16% in base shear and 3.89–4.05% in target displacement between concentrated and distributed hinge formulations. The development shown in Figure 2 therefore represents the modelled redistribution of inelastic deformation as X-direction lateral demand increases. This progression indicates that localized yielding gradually spreads across structural components while preserving an overall stable and interpretable nonlinear deformation pattern.

3.3. Plastic Hinge Development under Y-Direction Pushover Loading

Figure 3(a–h) presents the development of plastic hinge states in the ten-story RC building under pushover loading in the Y direction. The early analysis stages show limited hinge activation, with the nonlinear response concentrated in the lower stories. As lateral displacement increases, additional hinge locations appear in the lower and intermediate levels, while the upper stories remain less affected. This vertical distribution is consistent with the larger story shear and overturning demand that develop toward the base of a moment-resisting frame. The hinge pattern also indicates that yielding does not occur simultaneously throughout the building. Instead, local inelastic actions spread gradually as lateral demand increases. Hussein et al. (2021) observed similar sensitivity of hinge distribution in 30 reinforced concrete frame models analyzed by nonlinear static procedures, where changes in story height and span arrangement altered the location and sequence of plastic hinge formation. Rc et al. (2024) reported distinct X- and Y-direction hinge states in reinforced concrete buildings subjected to pushover analysis. Their results showed that hinge populations progressively moved from the A–B range toward B–IO, IO–LS, and more advanced performance states as displacement demand increased. Kuria and Kegyes-Brassai (2023) tracked 51 pushover iterations in an existing RC hospital building; column hinges first appeared at the fourth iteration, while beam yielding began at the fourteenth iteration. The progression visible in Figure 3(a–d) reflects spatial redistribution of inelastic demand rather than uniform stiffness loss over the structural height.

At the later stages shown in Figure 3(e–h), plastic hinge activity becomes more pronounced in the lower half of the frame. Several hinge markers progress from the initial B state toward the Immediate Occupancy range, while the upper stories exhibit fewer advanced hinge states. The displayed sequence does not show widespread concentration of hinges in the Collapse Prevention or post-C regions, although the precise state of each hinge should be confirmed from the numerical hinge table rather than from color inspection alone. Abass and Jarallah (2021) demonstrated that nonlinear hinge properties, plastic hinge length, and transverse reinforcement assumptions can modify the predicted capacity curve and hinge response of reinforced concrete frames. Their study compared four- and seven-story frames and emphasized the need to interpret hinge states with the selected nonlinear modelling parameters. Le and Pham (2024) reached a similar conclusion for a four-story reinforced concrete frame. They found that alternative concentrated and distributed hinge formulations produced differences of approximately 1.26–2.16% in base shear and 3.89–4.05% in target displacement. These modelling effects are relevant when Figure 3 is compared with the X-direction response in Figure 2. The Y-direction sequence retains the strongest concentration of nonlinear action in the lower and intermediate stories, while the spatial spread differs from the pattern observed under X-direction loading. This directional variation is consistent with the approximately 5% lower maximum base-shear capacity previously obtained for the Y direction. The relationship between local hinge progression and global Y-direction capacity response provides the basis for evaluating three-dimensional hinge distribution and the ATC-40 performance point in the subsequent structural performance assessment sections.

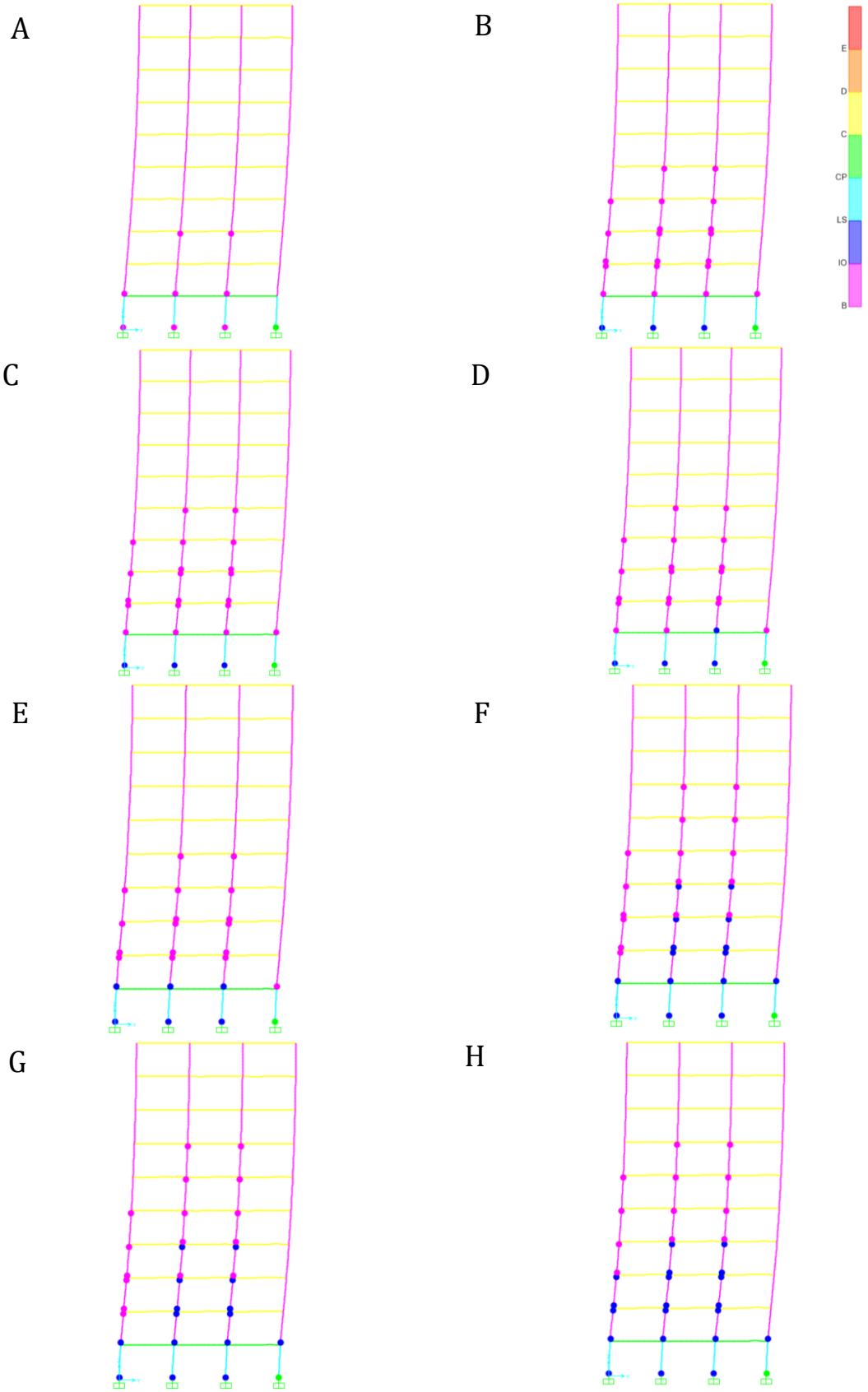


Figure 3. Evolution of plastic hinge states in the ten-story reinforced concrete building under nonlinear static pushover loading in the Y direction: (a) Step 1, (b) Step 2, (c) Step 3, (d) Step 4, (e) Step 5, (f) Step 6, (g) Step 7, and (h) Step 8

3.4. Three-Dimensional Plastic Hinge Distribution and Inelastic Response Mechanism

Figure 4 presents the three-dimensional distribution of plastic hinge states in the ten-story reinforced concrete building at a stage of nonlinear static pushover analysis. Unlike the two-dimensional frame views in Figures 2 and 3, the three-dimensional representation shows how inelastic actions are distributed over the building height and across frame lines. Plastic hinge markers are visible at numerous member-end locations, with more advanced color states concentrated mainly within the lower and intermediate stories. The upper stories remain dominated by the initial hinge range, which indicates lower local inelastic demand at the displayed structural state. This vertical concentration is mechanically consistent with the larger story shear and overturning effects expected near the base of a multistory frame. The pattern should not be interpreted as a collapse mechanism because Figure 4 does not show widespread hinge progression into the D–E or Beyond-E ranges. Hussein et al. [1] analyzed 30 reinforced concrete frame systems and examined how variations in span length and story height affected plastic-hinge distribution and the resulting failure mode. Their study also used the hinge pattern to identify the progression of nonlinear response during pushover loading. Kuria and Kegyes-Brassai [2] demonstrated that hinge formation can occur sequentially rather than simultaneously. Their existing RC hospital model required 51 pushover iterations, with the first column hinges appearing at iteration 4 at a load factor of 0.8641 and the first beam yielding occurring at iteration 14 at a load factor of 1.253. These numerical observations are comparable with the spatial progression visible in Figure 4, where the lower portion of the structural system exhibits a greater concentration of developed hinge states than the upper levels.

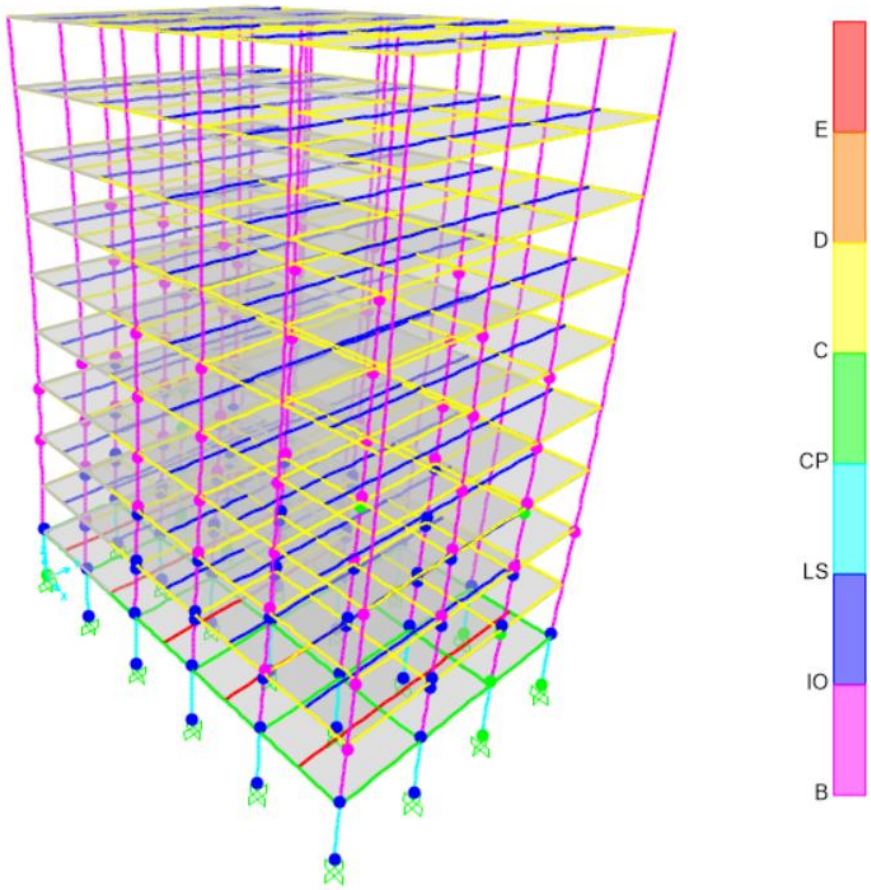
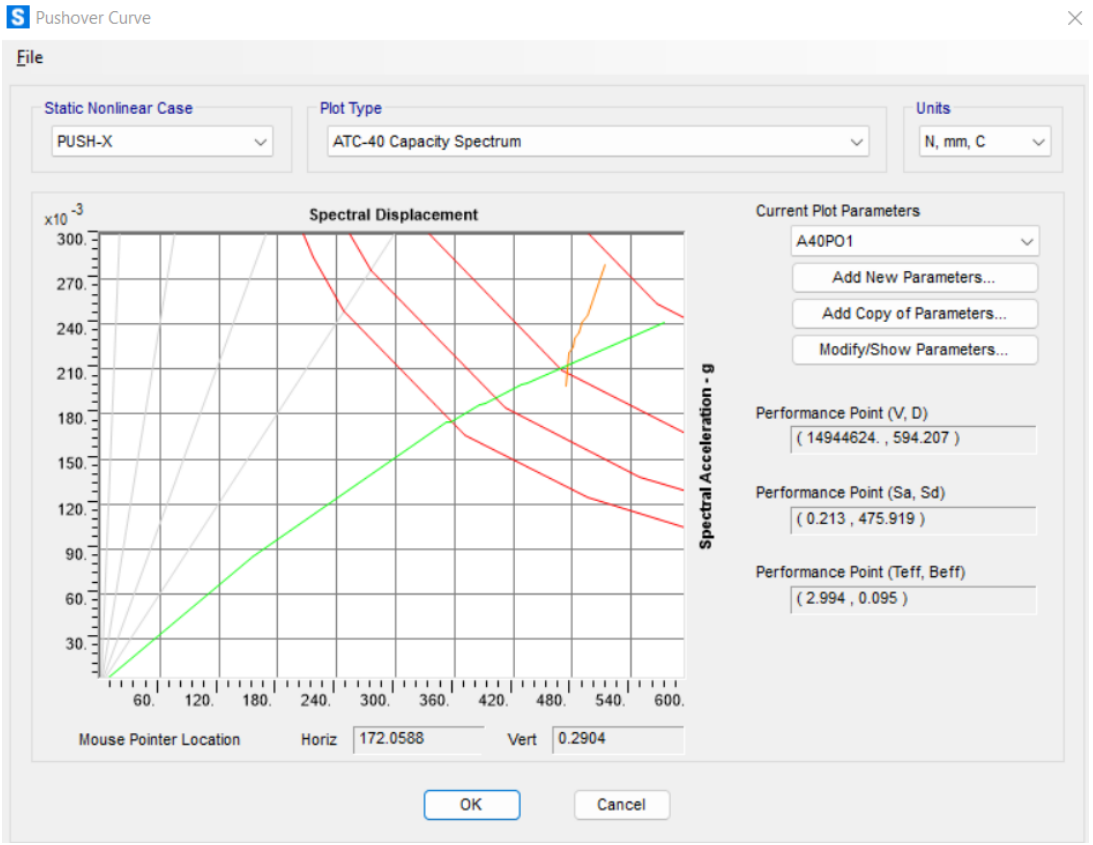


Figure 4. Three-dimensional view of plastic hinge formation and structural deformation of the ten-story reinforced concrete building under nonlinear static pushover loading

A



B

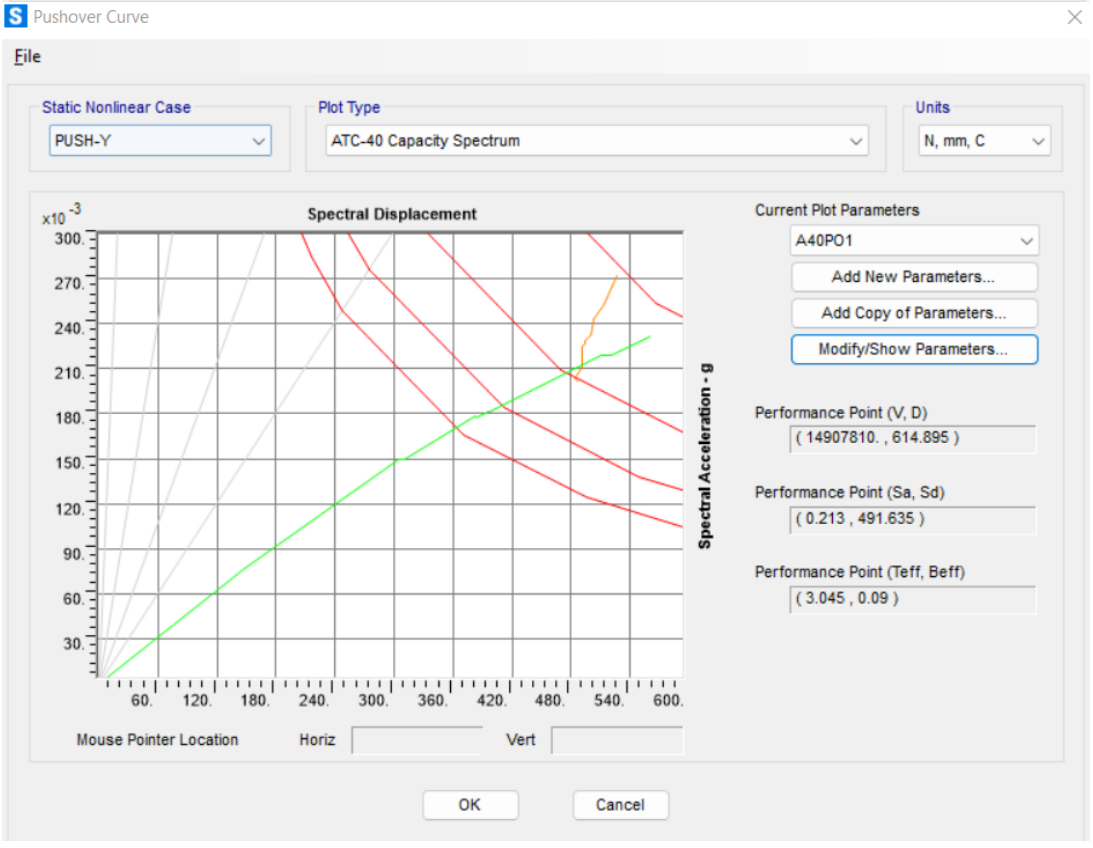


Figure 5. Determination of the seismic performance point using the ATC-40 capacity spectrum method: (a) pushover response in the X direction and (b) pushover response in the Y direction

The three-dimensional hinge pattern provides information on how local yielding contributes to the inelastic response discussed in Sections 3.1–3.3. In Figure 4, advanced hinge states are distributed over lower-story frames rather than being confined to an isolated vertical line. Such spatial spreading suggests that lateral deformation is resisted by several frame components, although the figure does not provide hinge counts or rotations needed to quantify this distribution. Mitropoulou et al. [3] performed sixteen nonlinear static analyses on a multistory RC building and reported that structural strengthening nearly doubled the base shear at the performance point while reducing the corresponding deformation by approximately 25–30%. Their results also showed that plasticization could shift between column and beam ends when stiffness and strength distributions were modified. Barbagallo et al. [4] compared lumped-plasticity and distributed-plasticity approaches through two three-dimensional RC building models. Both approaches produced similar assessments for structures with ductile response, whereas the lumped-hinge formulation produced more conservative estimates for systems characterized by lower ductility or brittle mechanisms. Shi et al. [5] also showed that plastic-hinge performance varies with structural configuration. Their study compared column orientations and story levels from the first through fifth floors using SAP2000 and ABAQUS and identified different nonlinear response characteristics across the investigated levels. The concentration of advanced states within the lower portion of Figure 4 is therefore treated as localized inelastic demand, while the corresponding seismic performance level is evaluated separately from the ATC-40 capacity spectrum in Section 3.5.

3.5. ATC-40 Performance Point and Seismic Performance Level

Figure 5(a) and Figure 5(b) present the ATC-40 capacity-spectrum assessment for the X and Y directions. The performance point is obtained from the intersection between structural capacity and seismic demand in acceleration–displacement response spectrum coordinates. In the X direction, Figure 5(a) gives a performance-point base shear of 14,944.624 kN at a monitored displacement of 594.207 mm. The corresponding spectral coordinates are Sa = 0.213 g and Sd = 475.919 mm, with an effective period of 2.994 s and an effective damping ratio of 9.5%. In the Y direction, Figure 5(b) gives a base shear of 14,907.810 kN at 614.895 mm displacement. The spectral displacement increases to 491.635 mm at the same spectral acceleration of 0.213 g, while the effective period reaches 3.045 s and the effective damping ratio is 9.0%. The difference in performance-point base shear between the two directions is only 36.814 kN, or about 0.25%, whereas the Y-direction displacement is 20.688 mm, or about 3.48%, greater than the X-direction value. This response indicates that both directions mobilize nearly comparable lateral resistance at the demand intersection, although the Y direction requires a larger deformation to reach that state. Getachew et al. [1] emphasized that performance-point displacement is a key demand parameter because member forces and deformations are evaluated at this displacement. Mahmood and Mohamad [2] also showed for a ten-story RC building that the estimated performance point can vary with the lateral load distribution adopted in pushover analysis.

The performance-level calculation associated with Figure 5 places both directions within the Damage Control range, which corresponds to SP-2 between Immediate Occupancy (SP-1) and Life Safety (SP-3) in ATC-40 terminology. This classification is consistent with the hinge development in Figures 2–4, where nonlinear activity spreads through the lower and intermediate stories without progression into the most severe hinge states. The result should be interpreted from global displacement demand and component response, rather than from the performance-point intersection alone. Pierre and Hidayat [3] reported an Immediate Occupancy classification when the maximum drift ratio of their RC structure was 0.00047, below the adopted limit of 0.005. Hutama [4] obtained ATC-40 performance indices of 0.00433 and 0.00408 in the X and Y directions for a hospital building, with both directions classified as Immediate Occupancy. A different response was reported by Sucipto et al. [5], who obtained capacity-spectrum displacements of 0.2022 m in the X direction and 0.1965 m

in the Y direction and classified the structure as Damage Control according to ATC-40, while the FEMA 440 procedure produced Life Safety. These results illustrate that performance classification depends on the calculated demand point, drift measure, structural properties, and assessment procedure. For the present building, the similar performance-point base shears indicate comparable demand-level resistance in both directions, while the larger Y-direction displacement and effective period reveal a directional difference in deformation response. The Damage Control range indicates that inelastic response has developed beyond Immediate Occupancy while remaining below the Life Safety performance state, subject to verification of the reported drift calculations against specified ATC-40 deformation limits.

4. Conclusion

The structural assessment shows that the ten-story reinforced concrete building provides adequate member strength and develops a stable nonlinear response under the evaluated seismic loading conditions. The beam flexural capacity reaches 186.96 kN·m compared with a factored moment demand of 64.92 kN·m, while the reduced column axial capacity reaches 6407.29 kN against an axial demand of 1627.27 kN. The pushover analysis indicates a maximum base shear of 17,110.19 kN at a roof displacement of 0.715 m in the X direction and 16,301.71 kN at 0.699 m in the Y direction, which gives approximately 5.0% higher lateral resistance in the X direction. Plastic hinges develop progressively within the lower and intermediate stories as lateral displacement increases, without widespread progression into the most severe hinge states at the evaluated stages. The ATC-40 capacity-spectrum assessment gives performance-point base shears of 14,944.62 kN and 14,907.81 kN in the X and Y directions, with corresponding monitored displacements of 594.21 and 614.90 mm. Both directions are classified within the Damage Control performance range between Immediate Occupancy and Life Safety. The study is limited to nonlinear static pushover analysis, which represents seismic demand through a prescribed lateral load pattern and cannot fully reproduce cyclic response, higher-mode interaction, record-to-record variability, or strength and stiffness degradation under actual earthquake ground motions. The member-capacity assessment is also based on the selected structural sections and modelling assumptions used in the analytical model. Further investigation is therefore recommended using nonlinear time-history analysis with a representative suite of ground-motion records. Sensitivity studies on hinge properties, material nonlinearities, geometric nonlinearities, soil–structure interaction, and modelling uncertainty are also required to verify the predicted performance point and directional seismic response of the building.

References

[1] L. S. Encalada, E. D. Muñoz, D. A. Sosa, M. N. Herrera, J. C. Velastegui and C. M. Gómez, “Seismic performance assessment of risk category III Ecuadorian buildings made of reinforced concrete frames and flat slabs”, *Structures*, vol. 87, Art. no. 111612, (2026), doi: 10.1016/j.istruc.2026.111612.

[2] M. Zameeruddin and K. K. Sangle, “Performance-based seismic assessment of reinforced concrete moment resisting frame”, *Journal of King Saud University - Engineering Sciences*, vol. 33, pp. 153-165, (2021), doi: 10.1016/j.jksues.2020.04.005.

[3] N. Fazarinc, A. Babič and M. Dolšek, “Parametric pushover curve model for seismic performance assessment of building stock”, *Bulletin of Earthquake Engineering*, vol. 22, pp. 1425-1449, (2024), doi: 10.1007/s10518-023-01821-9.

[4] A. Zendaoui, A. Kadid and D. Yahiaoui, “Comparison of different numerical models of RC elements for predicting the seismic performance of structures”, *International Journal of Concrete Structures and Materials*, vol. 10, no. 4, pp. 461-478, (2016), doi: 10.1007/s40069-016-0170-7.

[5] A. J. Pierre and I. Hidayat, "Seismic performance of reinforced concrete structures with pushover analysis", *IOP Conference Series: Earth and Environmental Science*, vol. 426, Art. no. 012045, (2020), doi: 10.1088/1755-1315/426/1/012045.

[6] A. Abd-Elhamed, S. Mahmoud and K. S. Alotaibi, "Nonlinear analysis of reinforced concrete buildings with different heights and floor systems", *Scientific Reports*, vol. 13, Art. no. 14949, (2023), doi: 10.1038/s41598-023-41656-7.

[7] M. Ariyanto, R. H. Purba and H. Riyanto, "Seismic response of reinforced concrete structures using pushover analysis with varying number of storeys", *Reka Buana: Jurnal Ilmiah Teknik Sipil dan Teknik Kimia*, vol. 11, no. 1, pp. 169-181, (2026), doi: 10.33366/rekabuana.v11i1.8330.

[8] M. M. Hussein, M. Gamal and W. A. Attia, "Seismic response modification factor for RC-frames with non-uniform dimensions", *Cogent Engineering*, vol. 8, no. 1, Art. no. 1923363, (2021), doi: 10.1080/23311916.2021.1923363.

[9] M. Zhang, R. Liu, Y. Li and G. Zhao, "Seismic performance of a corroded reinforce concrete frame structure using pushover method", *Advances in Civil Engineering*, vol. 2018, Art. no. 7208031, pp. 1-12, (2018), doi: 10.1155/2018/7208031.

[10] C. C. Mitropoulou, I. A. Naziris, N. A. Kallioras and N. D. Lagaros, "Optimized strengthening based on concrete jacketing for minimum eccentricity", *Frontiers in Built Environment*, vol. 8, Art. no. 856380, (2022), doi: 10.3389/fbuil.2022.856380.

[11] T. A. Le and N. H. Pham, "Effects of plastic hinge properties on nonlinear static analysis of reinforced concrete frames", in *Hydraulic and Civil Engineering Technology IX*, pp. 622-628, (2024), doi: 10.3233/ATDE241041.

[12] K. K. Kuria and O. K. Kegyes-Brassai, "Nonlinear static analysis for seismic evaluation of existing RC hospital building", *Applied Sciences*, vol. 13, no. 21, Art. no. 11626, (2023), doi: 10.3390/app132111626.

[13] H. A. Abass and H. K. Jarallah, "Development and verification of the capacity curve for two dimensional reinforced concrete moment-resisting frames system under earthquake loading", *Journal of Engineering*, vol. 27, no. 6, pp. 73-96, (2021), doi: 10.31026/j.eng.2021.06.06.

[14] F. Barbagallo, M. Di Domenico, M. Terrenzi, C. Cantagallo, E. M. Marino, P. Ricci, G. M. Verderame, G. Camata and E. Spacone, "Influence of the modelling approach on the seismic assessment of RC structures by nonlinear static analyses", *Soil Dynamics and Earthquake Engineering*, vol. 172, Art. no. 107970, (2023), doi: 10.1016/j.soildyn.2023.107970.

[15] M. Shi, M.-W. Choi, Y. Choi and S. Kang, "Influences of column orientations and story levels of the RC frames under nonlinear static analysis", *Architectural Research*, vol. 26, no. 4, pp. 127-138, (2024), doi: 10.5659/AIKAR.2024.26.4.127.

[16] K. Getachew, D.-H. Chen and G. Peng, "Seismic performance evaluation of RC frame designed using Ethiopian and Chinese seismic codes", *Advances in Civil Engineering*, vol. 2020, Art. no. 8493495, (2020), doi: 10.1155/2020/8493495.

[17] M. N. Mahmood and H. J. Mohamad, "Dynamic and pushover analysis of multi-storey reinforced concrete building using different load distribution pattern", *Journal of Applied Engineering Science*, vol. 20, no. 4, pp. 1325-1334, (2022), doi: 10.5937/jaes0-37318.

[18] B. P. Hutama, "Evaluasi kinerja bangunan Rumah Sakit Santa Maria Pemalang dengan non-linier static pushover analysis metode ATC-40 dan FEMA 440", *INERSIA: Informasi dan Ekspose Hasil Riset Teknik Sipil dan Arsitektur*, vol. 17, no. 2, pp. 118-129, (2021), doi: 10.21831/inersia.v17i2.25511.

[19] W. Sucipto, J. Tanijaya and H. T. Kalangi, "Analisis kinerja seismik struktur beton bertulang (Studi kasus: Tower 'A' Gedung Ciputra School of Business Makassar)", *Jurnal Media Teknik Sipil*, vol. 1, no. 1, pp. 16-26, (2023), doi: 10.56963/judiateks.v1i1.11.

[20] B. Rc, V. Rani, M. F. Suleiman, B. B. Biradar, R. Vyas, A. Ahmad and A. I. Shirkol, "Seismic performance evaluation and comparative study of reinforced concrete building on a sloped terrain with regular building by considering the effect of URM infill walls", *Buildings*, vol. 14, no. 1, Art. no. 33, (2024), doi: 10.3390/buildings14010033.

[21] Badan Standardisasi Nasional, *SNI 1726:2019: Tata Cara Perencanaan Ketahanan Gempa untuk Struktur Bangunan Gedung dan Nongedung*, Jakarta, Indonesia, (2019).

[22] Badan Standardisasi Nasional, *SNI 2847:2019: Persyaratan Beton Struktural untuk Bangunan Gedung dan Penjelasan*, Jakarta, Indonesia, (2019).

[23] H. Krawinkler and G. D. P. K. Seneviratna, "Pros and cons of a pushover analysis of seismic performance evaluation", *Engineering Structures*, vol. 20, no. 4-6, pp. 452-464, (1998), doi: 10.1016/S0141-0296(97)00092-8.

[24] X. Zhao, Y.-F. Wu, A. Y. T. Leung and H. F. Lam, "Plastic hinge length in reinforced concrete flexural members", *Procedia Engineering*, vol. 14, pp. 1266-1274, (2011), doi: 10.1016/j.proeng.2011.07.159.

[25] H. A. Safarizki, S. A. Kristiawan and A. Basuki, "Evaluation of the use of steel bracing to improve seismic performance of reinforced concrete building", *Procedia Engineering*, vol. 54, pp. 447-456, (2013), doi: 10.1016/j.proeng.2013.03.040.

[26] Applied Technology Council, *Seismic Evaluation and Retrofit of Concrete Buildings*, ATC-40, Vols. 1-2, Report No. SSC 96-01, Redwood City, CA, USA, November 1996.